

Investigation of the Role of Bicyclic Peroxy Radicals in the Oxidation Mechanism of Toluene

Adam W. Birdsall, John F. Andreoni, and Matthew J. Elrod*

Department of Chemistry and Biochemistry, Oberlin College, Oberlin, Ohio, 44074

Received: June 14, 2010; Revised Manuscript Received: August 31, 2010

The products of the primary OH-initiated oxidation of toluene were investigated using the turbulent flow chemical ionization mass spectrometry technique under different oxygen, NO, and initial OH radical concentrations as well as a range of total pressures. The bicyclic peroxy radical intermediate, a key proposed intermediate species in the Master Chemical Mechanism (MCM) for the atmospheric oxidation of toluene, was detected for the first time. The toluene oxidation mechanism was shown to have a strong oxygen concentration dependence, presumably due to the central role of the bicyclic peroxy radical in determining the stable product distribution at atmospheric oxygen concentrations. The results also suggest a potential role for bicyclic peroxy radical + HO₂ reactions at high HO₂/NO ratios. These reactions are postulated to be a source of the inconsistencies between environmental chamber results and predictions from the MCM.

Introduction

Aromatic compounds are among the key anthropogenic precursors that lead to the formation of both tropospheric ozone and secondary organic aerosol (SOA) pollution.^{1,2} With sources arising from automobile exhaust, petroleum refining processes, and industrial solvent evaporation, aromatic compounds (the most atmospherically abundant species are typically benzene, toluene, dimethylbenzenes, ethylbenzene, and trimethylbenzenes) can account for 20–40% of the total nonmethane hydrocarbon (NMHC) content of the atmosphere in urban areas.³ Due to their relatively high OH reactivity, aromatic compounds play an even larger role in photochemical air pollution than their atmospheric abundance would suggest.¹ Therefore, a detailed understanding of the role of aromatic compounds in the formation of tropospheric ozone and SOA air pollution is essential to the goal of improved air quality.

On the basis of the large body of experimental work on the photochemical oxidation of aromatic compounds, the Master Chemical Mechanism (MCM) has been developed to provide an explicit representation of the constituent reactions involved in the aromatic oxidation mechanism.⁴ However, there remain a number of key uncertainties, even for the well-studied toluene system. In particular, the MCM overpredicts ozone concentrations by 55% and underpredicts OH production by 44% in environmental chamber experiments meant to closely simulate atmospheric conditions for toluene oxidation.^{4,5} These outstanding issues are important as they directly hinder the MCM's ability to model the contributions of aromatic compounds to the problem of air pollution and, thus, the effort to construct effective regulatory policies to improve air quality.

The existence of conflicting experimental results concerning the nature of the constituent reactions of the mechanism have likely played a major role in predictive performance problems of the MCM. For example, it is uncertain whether observed oxidation products are the result of primary (a single OH reaction event) or secondary oxidation (two OH reaction events) in part because most experiments continuously produce OH in

the reaction system. In addition, most experimental methods use a photochemical OH source, which may inadvertently cause the photochemical degradation of the primary products of the aromatic oxidation mechanism. Therefore, it is of interest to use experimental methods in which the primary and secondary oxidation chemistry can be more tightly controlled in order to allow the primary and secondary steps to be definitively identified.

Regarding the predictive performance problems of the MCM with respect to environmental chamber data, it was suggested that the discrepancies could be explained if the MCM model was "...missing oxidation processes that produce or regenerate OH without or with little NO to NO₂ conversion".⁵ The role of NO in the aromatic oxidation mechanisms has been difficult to determine in part due to the experimental conditions most commonly used. In most of these experiments, OH itself was generated via photochemical reactions involving NO, and it was not possible to definitively identify products arising specifically from NO reactions. Consequently, it is desirable to apply experimental methods in which the NO levels can be varied independently of the OH levels, with NO-free experiments being of particular interest.

Finally, there is currently poor qualitative and quantitative agreement among the existing oxidation product studies for toluene.^{6–21} There have been a wide variety of products detected using the various experimental methods formed from the oxidation of toluene, including ring-retaining species such as benzaldehyde and cresol as well as more highly oxidized species that result from the scission of the aromatic ring such as glyoxal and methylglyoxal. The latter species are postulated to form via a bicyclic (formed by the addition of O₂ as a bridging substituent) peroxy radical (formed by the addition of a second O₂ moiety) intermediate.^{5,22} However, this important species has yet to be experimentally detected. In previous low oxygen concentration experiments performed in our lab,⁸ the concomitant lack of observation of the bicyclic peroxy radical intermediate and ring scission products was rationalized through the existence of an equilibrium process for the addition of the second O₂ moiety that favors the bicyclic peroxy radical intermediate only at very high oxygen concentrations.^{23,24} Because it appears

* To whom correspondence should be addressed. E-mail: mjelrod@oberlin.edu.

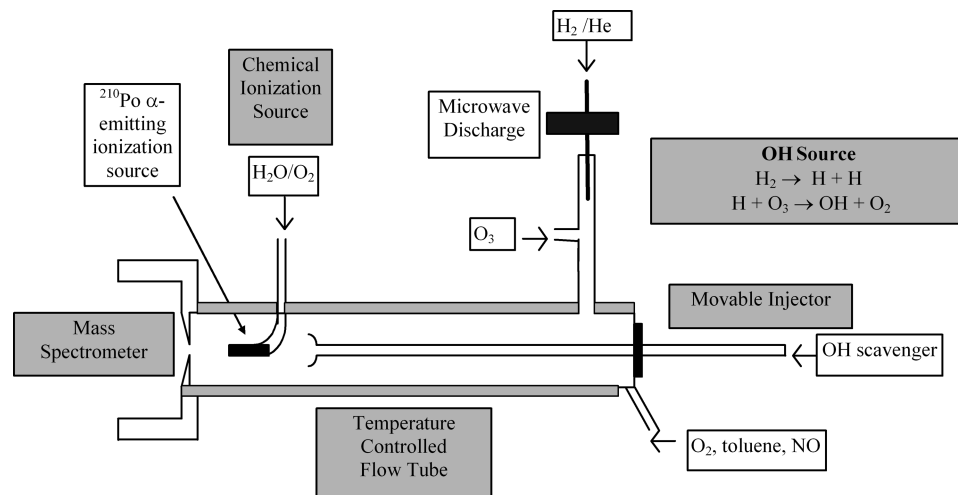


Figure 1. Experimental apparatus.

that the toluene oxidation mechanism depends sensitively on the concentrations of several reactant species, it is of interest to apply experimental methods in which many of the important oxidation intermediates and products can be simultaneously observed as a function of various reactant concentration levels, with the direct observation of the role of the bicyclic peroxy radical intermediate as a particularly important goal.

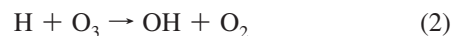
This article describes the identification of primary oxidation system intermediates and the detection and quantification of stable primary oxidation products for toluene via the turbulent flow chemical ionization mass spectrometry (TF-CIMS) technique. In particular, the CIMS approach allowed for a more complete identification of the reaction system species, and the TF method provided the facility to separately control OH, NO, and O₂ levels in the system as well as the ability to perform total pressure dependence measurements.

Experimental Section

Turbulent Fast Flow Tube. A schematic of the experimental apparatus is given in Figure 1. The main flow tube was 100 cm in length and constructed with 2.2 cm inner diameter Pyrex tubing. A large flow of variable amounts of oxygen and nitrogen carrier gas (30 STP L min⁻¹) was introduced at the rear of the flow tube to ensure turbulent flow conditions (Reynolds Number ≈ 2100 for most experiments). The reactants necessary for the production of OH radicals were prepared in a 20 cm long, 1.25 cm inner diameter side arm, while toluene and NO were added to the rear of the flow tube, as shown in Figure 1. This arrangement allowed for the separate synthesis of OH radicals but allowed all other reactants to be simultaneously present at the rear of the flow tube. For experiments involving the OH radical scavengers, the scavenger species were introduced into the main flow tube through an encased moveable injector. The encasement was made of corrugated Teflon tubing and allowed the injector to be moved to various injector positions (“time = zero” injector position is set just upstream of the ionization source) without breaking any vacuum seals. A fan-shaped Teflon device was placed at the end of the injector to enhance turbulent mixing. All gas flows were monitored with calibrated mass flow meters. A polonium-210 (²¹⁰Po) α-particle-emitting ionization source was placed between the flow tube and the entrance to the CIMS. Flow tube pressure and temperature were measured upstream of the ionization source. Pressure was measured using a 0–1000 Torr capacitance manometer. Temperature was determined using Cu-constantan thermocouples and was in the

range of 296–298 K for all experiments. Most of the flow tube gases were removed at the CIMS inlet using a 31 L s⁻¹ roughing pump.

OH Source. In order to ensure that the OH synthesis method did not introduce undesired secondary chemistry, several different OH sources were tested. The F + H₂O (used in our previous study of toluene oxidation⁸), H + NO₂, and H + O₃ sources were tested. The same major toluene oxidation products were observed for all three sources. However, the H + O₃ source was selected as the superior source because it was NO_x-free (important for assessing the NO dependence of the toluene oxidation mechanism) and H₂O-free (allowed more consistent performance of the proton-transfer chemical ionization mass spectrometer). The H + O₃ source utilizes the microwave-discharge-initiated dissociation of H₂, followed by reaction with O₃



A dilute mixture of He/H₂ was passed through a microwave discharge, produced by a Beenakker cavity operating at 50 W, to create hydrogen atoms (reaction 1). The dilute mixture was obtained by combining a 5.0 STP L min⁻¹ flow of ultrahigh purity helium (99.999%) with a 1.0 STP mL min⁻¹ flow of a 0.1–1.0% H₂ (99.9%)/He mixture. The 5.0 STP L min⁻¹ helium flow was first passed through a silica gel trap immersed in liquid nitrogen to remove any possible impurities. The hydrogen atoms were then injected into the flow tube side arm and mixed with a flow of O₃ entrained in He. Ozone was produced in a commercial ozonizer and stored on a silica-gel-filled trap at -78 C. O₃ was introduced into the system by passing a 1–4 STP mL min⁻¹ flow of He through the trap. Ozone partial pressures were determined by UV absorbance at 254 nm in a 1 cm flow-through quartz cuvette. Because O₃ was in great excess in the side arm ([O₃] = ~2 × 10¹³ molecules cm⁻³) and the H + O₃ reaction is very fast (2.9 × 10⁻¹¹ cm³ molecule⁻¹ s⁻²),²⁵ the OH-producing reaction had a very short lifetime of about 2 ms, thus ensuring that all hydrogen atoms were quickly consumed (the minimum side arm residence time for OH is about 20 ms).

Toluene Species. C₆H₅CD₃ (or one of the other commercially available toluene isotopes, C₇H₈ or C₇D₈) was added to the rear of the flow tube as a 1% mixture in N₂. The typical toluene

concentration for these experiments was 1×10^{13} molecules cm^{-3} . Using the known OH + toluene rate constant of about 6×10^{-12} $\text{cm}^3 \text{ molecule}^{-1} \text{ s}^{-1}$,²⁵ OH has a lifetime of about 17 ms under these conditions to produce the toluene–OH adduct, which is short compared to the 100 ms main flow tube residence time for toluene. These conditions ensured that the dominant fate of OH was reaction with toluene (the primary oxidation process of interest).

O₂ Dependence Studies. Oxygen concentrations were varied by adjusting the fraction of the 30 STP L min^{-1} carrier gas flow that was comprised of oxygen. At a total pressure of 200 Torr and with the carrier gas flow comprised entirely of oxygen, the main flow tube oxygen concentration was nearly that of the atmosphere at 760 Torr ($[\text{O}_2] = 5 \times 10^{18}$ molecules cm^{-3}). Therefore, the O₂ dependence studies were carried out at 200 Torr total pressure, so that O₂ concentrations as high as atmospheric levels could be accessed. For other experiments carried out at pressures greater than 200 Torr, the oxygen component of the carrier gas flow was adjusted to maintain a total oxygen concentration of 5×10^{18} molecules cm^{-3} .

NO Dependence Studies. NO [$0-2 \times 10^{13}$ molecules cm^{-3}] was introduced into the main flow tube as a 2% NO/N₂ mixture at the same injection point as toluene. The mixture was first passed through a silica gel trap held between -20 and -30 °C to remove any traces of NO₂ impurities. Negligible amounts of NO₂ impurities were observed using the CIMS technique.

Pressure Dependence Studies. The pressure was varied between 100 and 500 Torr by adjusting the roughing pump speed. Therefore, as the pressure was increased, the turbulent flow velocity proportionally decreased.

Initial OH Dependence Studies. By varying the amount of H₂ flow through the microwave discharge, the initial OH radical concentrations were varied. The approximate OH concentrations at each H₂ flow setting were estimated by several indirect methods, which are described below.

OH Scavenger Studies. *trans*-2-Butene [$\sim 1 \times 10^{13}$ molecules cm^{-3}], which is known to efficiently form peroxy radicals in the presence of OH and O₂,²⁶ was introduced to the main flow tube as a 10% *trans*-2-butene/N₂ mixture through the moveable injector. Although the concentrations of *trans*-2-butene and toluene were similar in this experiment, the OH + 2-butene reaction has a rate constant that is about 10 times larger than that of the OH + toluene reaction.²⁵ Therefore, the *trans*-2-butene species outcompeted toluene for OH under these conditions.

CIMS Detection. The chemical ionization reagent ions were produced using a commercial ²¹⁰Po α -particle emitting ionization source consisting of a hollow cylindrical (69 by 12.7 mm) aluminum body with 10 mCi (3.7×10^8 disintegrations s^{-1}) of ²¹⁰Po coated on the interior walls. All oxygenated organic species were detected using a proton-transfer CIMS scheme. The H⁺(H₂O)_{*n*} ions were produced by passing a large O₂ flow (7 STP L min^{-1}) through the ionization source, with H₂O impurities being sufficiently abundant to produce an adequate amount of reagent ions. The predominant species detected were the protonated (and partially hydrated) analogues of the neutral precursor oxygenated organic compounds. No fragment ions were detected. Toluene was detected with a C₄H₉⁺-adduct-forming CIMS scheme. C₄H₉⁺ reagent ions were produced by combining a large flow of N₂ (7 STP L min^{-1}) with a 12 STP mL min^{-1} flow of isobutane and passing the mixture through the ionization source. The predominant species detected was C₇H₈–C₄H₉⁺. OH and HO₂ were detected via SF₆[–] chemical ionization reactions, with OH[–] and SF₄O₂[–] as the detected ions

for each species, respectively.²⁷ SF₆[–] reagent ions were produced by combining a large flow of N₂ (7 STP L min^{-1}) with a 1 STP mL min^{-1} flow of 10% SF₆/N₂ and passing the mixture through the ionization source. Ions were detected with a quadrupole mass spectrometer housed in a two-stage differentially pumped vacuum chamber. Flow tube gases (neutrals and ions) were drawn into the front chamber through a charged 0.1 mm aperture. The front chamber was pumped by a 6 in. 2400 L s^{-1} diffusion pump. The ions were focused by three lenses constructed from 3.8 cm inner diameter and 4.8 cm outer diameter aluminum gaskets and then entered the rear chamber through a skimmer cone with a charged 1.0 mm orifice. The skimmer cone was placed approximately 5 cm from the front aperture. The rear chamber was pumped by a 250 L s^{-1} turbomolecular pump. After the ions had passed through the skimmer cone, they were mass filtered and detected with a quadrupole mass spectrometer.

Relative Product Yield Studies. The relative product yield is defined as the flow tube concentration of the species of interest divided by the sum of the flow tube concentrations of all measured products. Therefore, the relative yield % is defined as follows

$$\text{Relative yield \% product } i = \frac{[\text{product } i]}{\sum_j^n [\text{product } j]} \times 100 \quad (3)$$

This quantity requires the absolute concentrations of product species to be determined. Calibration curves for authentic samples of the products benzaldehyde and *o*-cresol were constructed by flowing a known concentration of each substance into the flow tube and measuring the CIMS response. As extensively discussed in our earlier study on the toluene oxidation system,⁸ because all other major products of the toluene oxidation system have either hydroxyl or carbonyl groups as the targets of the proton-transfer CIMS reactions, it is reasonable to use the *o*-cresol or benzaldehyde (or the more convenient octanal) CIMS response factors, respectively, as proxy CIMS response factors for the calibration of species for which authentic samples are not available. An upper limit (as will be discussed later, OH is also believed to be generated by the toluene oxidation process) approximation to the initial OH radical concentration for a particular experiment was calculated by assuming a stoichiometric equivalence between the initial OH concentration and the total amount of toluene products quantified.

Absolute Product Yield Studies. The absolute product yield is defined as the flow tube concentration of the species of interest divided by the total amount of reacted toluene precursor. The latter quantity can be determined by measuring the difference in the toluene flow tube concentrations with the OH source on and off. Since the toluene concentrations for the conditions with the OH source off are simply calculated from the flow conditions, the amount of reacted toluene precursor is simply calculated from the ratio of the CIMS signal for the two conditions, multiplied by the OH source off toluene flow tube concentration

$$[\text{reacted toluene}] = \left[1 - \frac{(\text{toluene CIMS signal})_{\text{OH source on}}}{(\text{toluene CIMS signal})_{\text{OH source off}}} \right] \times [\text{toluene}]_{\text{OH source off}} \quad (4)$$

The method of Noda et al. was also employed in the effort to quantify the amount of reacted toluene.⁷ This method uses the reactive loss of 1,3,5-trimethylphenol (TMP) as a tracer of OH reactivity, and the known OH rate constants for TMP and toluene are then used to calculate the total amount of reacted toluene.

Once the amount of reacted toluene is determined, the absolute yield % is calculated as follows

$$\text{Absolute yield \% product } i = \frac{[\text{product } i]}{[\text{reacted toluene}]} \times 100 \quad (5)$$

Results and Discussion

Detection of OH and HO₂. SF₆⁻ CIMS methods revealed that the OH source also produces some HO₂. HO₂ is likely produced via the H + O₂ reaction in the side arm, with O₂ arising from the decomposition of O₃ in the silica gel trap and in the tubing from the trap to the side arm. When toluene is added to the system under NO_x-free conditions, HO₂ levels are observed to increase. Under the same conditions of added toluene, OH levels are observed to decrease, but they do not drop to background levels, as would be expected given the short OH lifetime with respect to toluene. Considering the persistence of OH under these conditions, it is clear that the toluene oxidation system is regenerating OH. Unfortunately, absolute OH and HO₂ concentrations could not be determined via the OH + NO₂ → HNO₃ and HO₂ + NO → NO₂ + OH titration and calibration techniques, respectively, because of the interference of high levels of O₃ with the CIMS detection schemes for HNO₃ and NO₂. However, the indirect methods described in the Absolute Product Yield Studies section indicate that, under the usual OH source conditions, the initial OH concentration was on the order of 2 × 10¹¹ molecules cm⁻³. The OH production rate from the toluene oxidation system was quantified via a scavenger approach, as will be discussed below.

Identification of Toluene Oxidation Products. Several major products from the primary oxidation of toluene were identified based on CIMS spectra collected for OH + C₇H₈, OH + C₆H₅CD₃, and OH + C₇D₈ under NO_x-free conditions. The OH + C₆H₅CD₃ experiments were particularly useful as this system was characterized by the largest number of products with unique *m/z* ions in the proton-transfer CIMS spectrum. The products were identified according to the correspondence between the protonated (and, in some cases, also hydrated) ions and the neutral oxidation products.

In our previous work on the toluene system for NO_x-free conditions,⁸ we used relatively low O₂ concentrations (about 1 × 10¹⁶ molecules cm⁻³) and reported the observation of four major products (shown in Figure 2), benzaldehyde, cresol, methylhexadienedial, and methylhexenedial epoxide (shorthand, noted as epoxide). The present experiments were performed somewhat differently than those reported in Baltaretu et al.; (1) an H + O₃ source was used (as opposed to F + H₂O) to produce OH; (2) in order to minimize reactant concentrations and possible side reactions, the OH + toluene reaction was initiated in the main flow tube (as opposed to the side arm); and (3) most of the experiments were carried out at 200 Torr total pressure (as opposed to 100 Torr) to allow the oxygen concentrations to be varied all the way up to atmospheric levels (5 × 10¹⁸ molecules cm⁻³). Despite these differences in the experimental methods, the same four major products were observed in the present experiments at low O₂ concentrations.

However, two additional minor products were detected. In their study of the cresol-producing pathway in the OH-initiated oxidation of toluene, Noda et al. have reported that toluene can also undergo a dealkylation reaction (shown at the top of Figure 2) that produces phenol.⁷ Noda et al. found that the cresol to phenol ratio was about 5:1. We found a very similar result, with our cresol to phenol ratio determined to be about 4:1. In addition, our use of C₇D₈ (and the normal isotope of OH) in some experiments allowed us to further investigate the nature of the cresol-forming mechanism. Glowacki et al. proposed that two cresol-forming pathways are possible for toluene; (1) O₂ can directly abstract the hydrogen atom from the toluene ring in the toluene–OH adduct, which produces HO₂ and restores the aromaticity of the toluene ring, and (2) the toluene–OH–O₂ adduct can undergo an intramolecular reaction in which the hydrogen atom from the OH group is abstracted, followed by an intramolecular hydrogen atom transfer from the ring back to the oxygen atom, which also produces HO₂ and restores the aromaticity of the toluene ring.²² For the case of C₇D₈ + OH, the first mechanism will produce C₇D₇OH + DO₂, while the second mechanism will produce C₇D₇OD + HO₂, which are distinguishable species in our CIMS detection method. We find that that C₇D₇OH and C₇D₇OD are produced in a ratio of about 3:1, suggesting that both pathways are important but also indicating the dominance of the first mechanism in the production of cresol from the OH-initiated oxidation of toluene, as proposed in the theoretical work of Frankcombe.²⁸

For NO_x-free experiments carried out at atmospheric O₂ concentrations, many additional products were identified. The appearance of additional products at high O₂ levels is rationalized by the formation of a bicyclic peroxy radical (shown at the bottom of Figure 2, with the subsequent reactions that this species can undergo shown in Figure 3). In particular, butenedial and methylbutenedial (produced from other bicyclic peroxy radical isomers and/or OH attack at non-ortho positions (not shown in Figures 2 and 3)) were observed as major products, as well as several minor bicyclic species, including the bicyclic peroxy radical intermediate itself. To the best of our knowledge, this is the first experimental detection of this previously postulated key toluene oxidation intermediate. In the C₆H₅CD₃ experiments, the protonated bicyclic peroxy radical is detected at a unique *m/z* (177 amu), but the protonated bicyclic peroxide and protonated bicyclic carbonyl monohydrate species have a *m/z* coincidence at 178 amu (the *m/z* coincidence problem is identical in the C₇H₈ system). Very small signals for the bicyclic alcohol species were detected in the C₆H₅CD₃ system, but no reproducible signal could be detected at the analogous *m/z* ratios for the C₇D₈ system. Therefore, no quantitative yields are reported for the bicyclic alcohol species. Due to fewer *m/z* coincidences for other toluene oxidation products, the C₆H₅CD₃ system was used in the determination of quantitative product yields, with the total yield due to both the bicyclic peroxide and the bicyclic carbonyl species reported as a single “bicyclic” yield value. However, since the bicyclic peroxide and the bicyclic carbonyl species are not *m/z* coincident for the C₇D₈ system, some experiments were performed with C₇D₈ in order to partition the bicyclic yield value from the C₆H₅CD₃ into its bicyclic peroxide and bicyclic carbonyl components. From these experiments, it was estimated that roughly 25% of the bicyclic product observed in the C₆H₅CD₃ experiments was due to the presence of the bicyclic peroxide compound, with the balance due to the presence of the bicyclic carbonyl species. The definitive identification of methylglyoxal (the assumed product partner of butenedial) and glyoxal (the assumed product partner

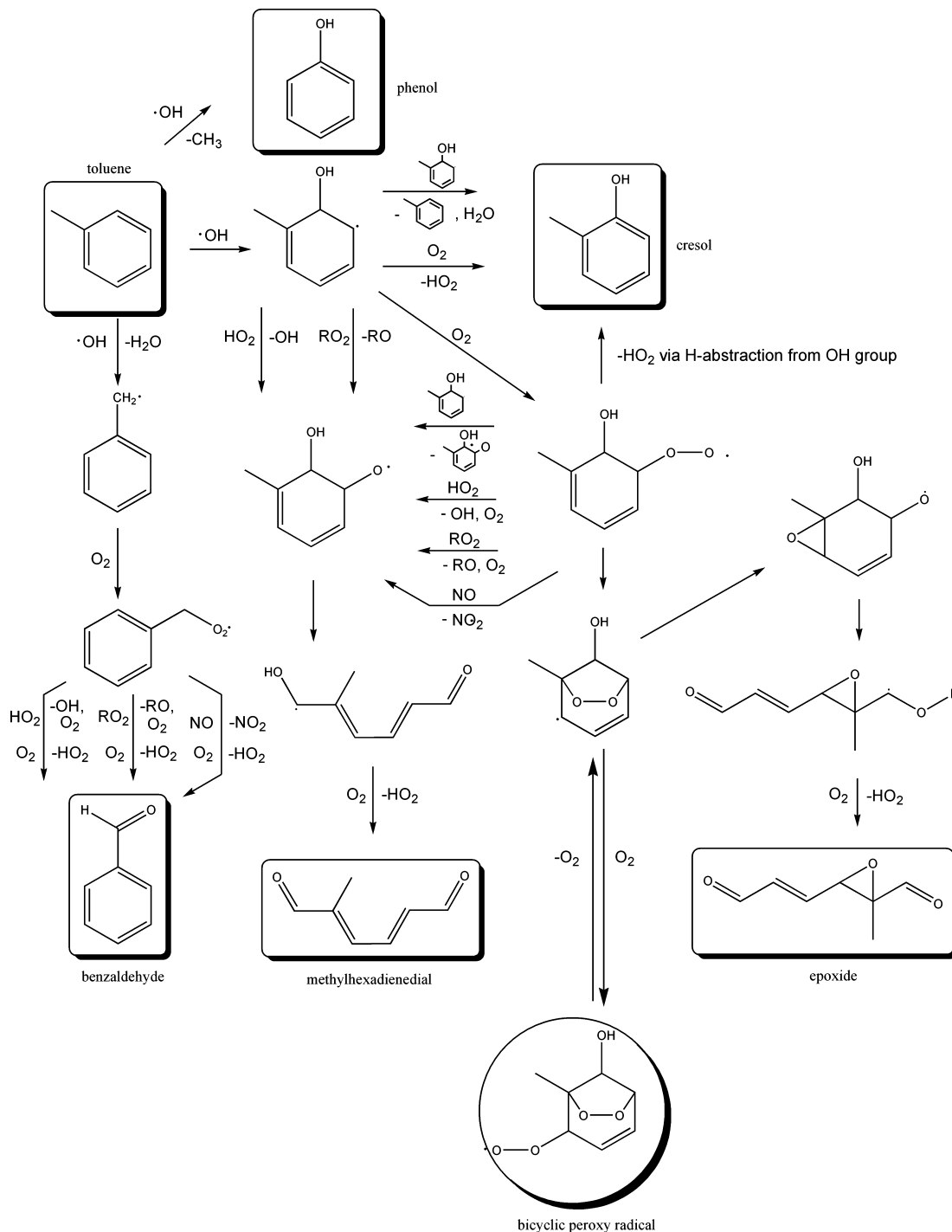


Figure 2. Low $[\text{O}_2]$ pathways in the primary OH-initiated oxidation of toluene.

of methylbutenedial for non-ortho OH attack) was stymied by several m/z coincidences, some of which were also reported by Zhao et al.,²⁹ who used similar CIMS detection techniques. Typical total identified product concentrations were about 2×10^{11} molecules cm^{-3} . The main sources of error in the product yield measurements were run to run variability ($\sim 20\%$, presumably due to slightly different flow tube conditions) and CIMS response factor variability ($\sim 20\%$).

Oxygen Dependence of Relative Product Yields. Figure 4 shows the relative product yield results for the O_2 dependence experiments under NO_x -free conditions at a total pressure of 200 Torr. As discussed above, at low O_2 concentrations, the stable species shown in Figure 2 are dominant, but at higher O_2 concentrations (but still significantly below atmospheric O_2

concentrations), the species shown in Figure 3 become much more important. In particular, while the methylhexadienedial product is still detectable at atmospheric O_2 concentrations, the methylbutenedial product has supplanted it as the dominant toluene oxidation product. Because the species in Figure 2 (with the exception of cresol and phenol) show a negative O_2 dependence, while the species in Figure 3 show a positive O_2 dependence, it seems quite clear that overall O_2 dependence is explained by the rising concentration (and reactivity) of the bicyclic peroxy radical intermediate as O_2 levels are increased. The persistence of the methylhexadienedial and epoxide species at the highest O_2 concentrations (where the O_2 dependence of the bicyclic peroxy intermediate derived species have plateaued)

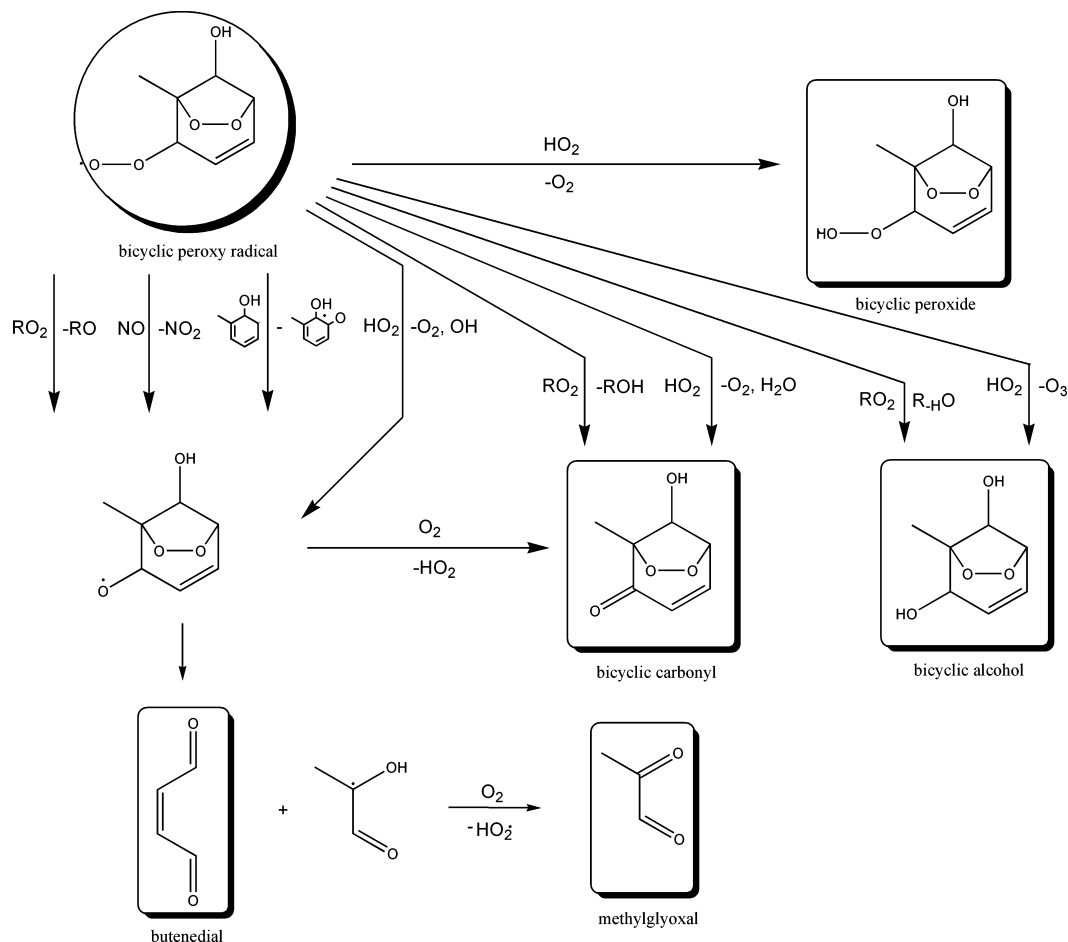


Figure 3. Bicyclic peroxy radical dependent pathways in the primary OH-initiated oxidation of toluene.

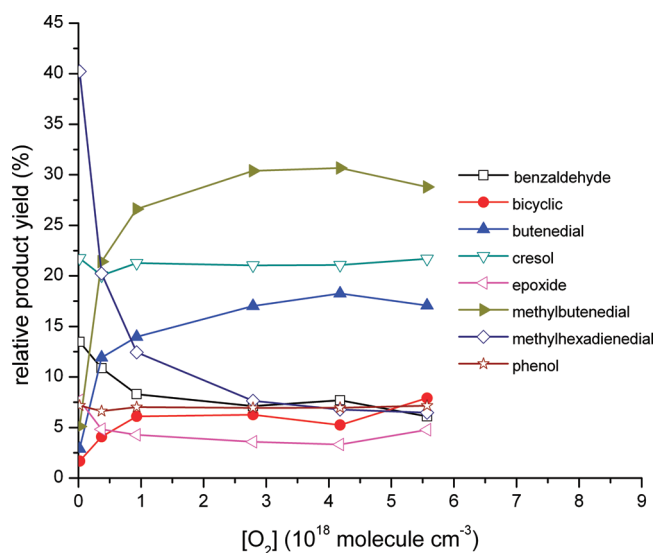


Figure 4. NO_x -free oxygen concentration dependence of toluene oxidation product yields at 200 Torr.

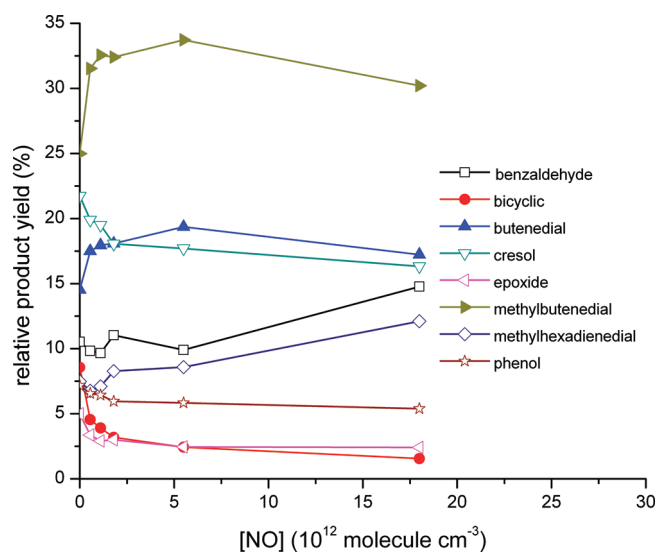


Figure 5. NO concentration dependence of toluene oxidation product yields at 200 Torr and $[\text{O}_2] = 5 \times 10^{18}$ molecules cm^{-3} .

suggests the possibility that these species might have minor production pathways via the bicyclic peroxy intermediate as well.

NO Dependence of Relative Product Yields. Figure 5 shows the relative product yield results for the NO dependence experiments at an O_2 concentration of 5×10^{18} molecules cm^{-3} and a total pressure of 200 Torr. For the species shown in Figure 2, adding NO increases the relative product yield of methylhexadienedial (a result previously observed by Berndt and Boge

in the benzene system³⁰) and benzaldehyde, while the relative product yield of the other species declines with increased NO concentration (this relative decline is mostly likely due to the increased absolute yields of the products that are enhanced at high NO). However, the more interesting NO dependence concerns the species shown in Figure 3. Increased NO concentrations favor the formation of the butenedial and methylbutenedial species, while the ring-retaining bicyclic species (including the bicyclic peroxy radical itself) are suppressed by high

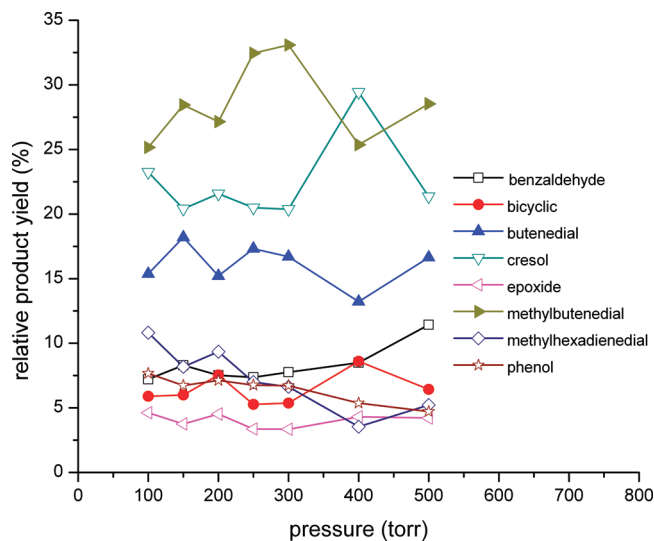


Figure 6. NO_x -free pressure dependence of toluene oxidation product yields (for pressures less than 200 Torr, $[\text{O}_2] = 0.85 \text{ [M]}$; for pressures of 200 Torr or greater, $[\text{O}_2] = [\text{O}_2]_{\text{atmosphere}} = 5 \times 10^{18} \text{ molecules cm}^{-3}$).

levels of NO. From Figure 5, it is clear that at a NO concentration of about $5 \times 10^{11} \text{ molecules cm}^{-3}$, the kinetic pathways for the ring-retaining bicyclic species are competitive with the kinetic pathways for the formation of (additional) butenedial and methylbutenedial. Assuming a typical value for the $\text{RO}_2 + \text{NO}$ rate constant ($1 \times 10^{-11} \text{ cm}^3 \text{ molecule}^{-1} \text{ s}^{-1}$),²⁶ this suggests that the lifetimes of the reactions that produce the ring-retaining bicyclic species are on the order of 200 ms under these conditions.

Pressure Dependence of Relative Product Yields. Figure 6 shows the relative product yield results for the pressure dependence experiments under NO_x -free conditions. For the experiments between 100 and 200 Torr total pressure, the O_2 concentrations were equal to 0.86 of the total number density (14% of the flow was helium, and the balance was oxygen). For experiments above 200 Torr, the O_2 concentrations were fixed at $5 \times 10^{18} \text{ molecules cm}^{-3}$ by adding N_2 to the carrier gas flow. No experiments were performed above 500 Torr because of the degrading CIMS detection sensitivity as a function of pressure. Figure 6 provides no definitive indication of a pressure-dependent effect for the formation of any of the observed products.

Initial Radical Concentration Dependence of Relative Product Yields. The initial OH concentration was varied by changing the flow of H_2 gas in the OH source, which directly affected the initial concentration of the toluene radical intermediates and the amounts of final products eventually formed. Therefore, the sum of the concentrations of the observed final products can be used as a proxy for the initial radical concentrations. Figure 7 shows the relative product yield results for the initial radical dependence experiments under NO_x -free conditions at an O_2 concentration of $5 \times 10^{18} \text{ molecules cm}^{-3}$ and a total pressure of 200 Torr. Under NO_x -free conditions, according to the mechanism outlined in Figures 2 and 3, most major products are expected to be characterized by kinetic behavior that is second order in OH-produced intermediates (such as RO_2 and HO_2), and thus, the relative yields of products should not be affected by the initial radical dependence. However, Figure 2 indicates that the cresol and epoxide products could potentially be suppressed at high radical concentrations if their common intermediate (the nonbicyclic peroxy radical)

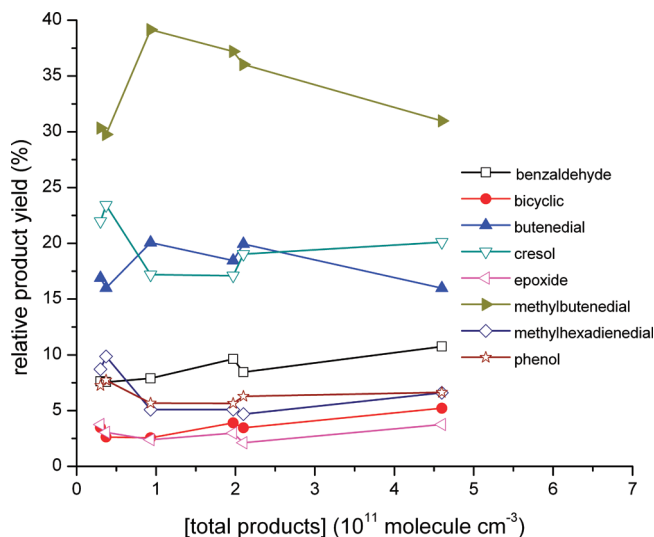


Figure 7. NO_x -free total products (initial OH radical) concentration dependence of toluene oxidation product yields at 200 Torr and $[\text{O}_2] = 5 \times 10^{18} \text{ molecules cm}^{-3}$.

were to undergo radical reactions to form the methylhexadienedial product rather than undergo a unimolecular or bimolecular (with O_2) reaction to form cresol or epoxide. While the cresol and epoxide yields are perhaps somewhat lower at the lowest initial radical concentrations (as shown in Figure 7), the measurements at very low initial radical concentrations were characterized by higher uncertainty due to the fact that several of the observed species had concentrations near the detection limit of the CIMS method. Therefore, it is difficult to make any conclusions from the initial radical concentration experiments.

OH Scavenger Studies. The scavenger experiments were carried out under NO_x -free conditions at an O_2 concentration of $5 \times 10^{18} \text{ molecules cm}^{-3}$ and a total pressure of 200 Torr, with the *trans*-2-butene scavenger added at a position downstream of the toluene injection point (50 ms) such that the initial OH + toluene reaction (lifetime = 17 ms) has largely gone to completion. Under the conditions used, the lifetime of OH with respect to *trans*-2-butene was only 2 ms; therefore, OH was virtually instantaneously converted to the *trans*-2-butene hydroxy peroxy radical. Using the CIMS response factor for a similar hydroxy species (cresol), the absolute concentrations of the *trans*-2-butene hydroxy peroxy radical were determined. A plot of the time-dependent behavior (relative to the *trans*-2-butene injection) of the *trans*-2-butene hydroxy peroxy radical concentration is depicted in Figure 8. Assuming a stoichiometric equivalence between the *trans*-2-butene hydroxy peroxy radical and OH, the data in Figure 8 indicate a OH production rate of about $1 \times 10^{11} \text{ molecules cm}^{-3} \text{ s}^{-1}$.

Absolute Product Yields. The absolute product yields were estimated for some experiments using the two methods described in the Experimental Section. The toluene depletion method, used in our previous study of the oxidation of toluene,⁸ was less reliable in the present experiments because of the smaller fraction of toluene reacted (this was a result of our efforts to use smaller initial radical concentrations more representative of atmospheric conditions). Nonetheless, this method indicated that between 50 and 100% of the reacted toluene had been accounted for in the observed products. The method of Noda et al.⁷ generally indicated that 100% of the reacted toluene had been accounted for. Because of the large uncertainties in the absolute product yield values for the present experiments, we report only relative yield values here but note that the absolute

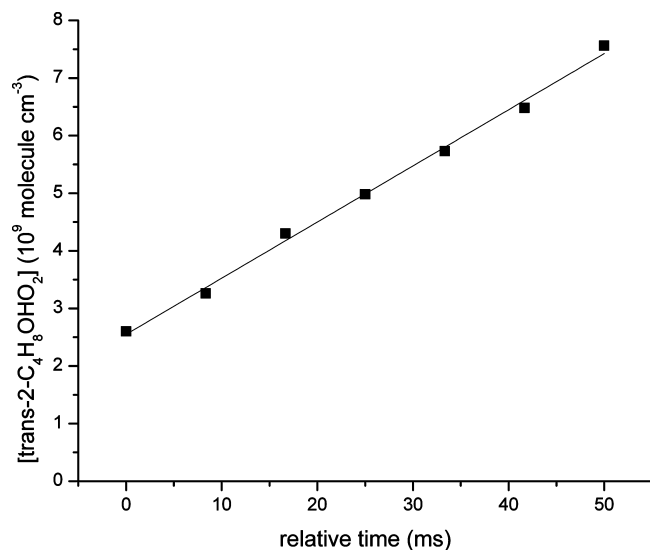


Figure 8. NO_x-free OH scavenger kinetics at 200 Torr and [O₂] = 5 × 10¹⁸ molecules cm⁻³.

yield data do seem to indicate that we have identified and quantified the majority of the toluene oxidation product mass.

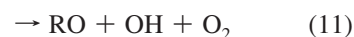
Implications for the Toluene Oxidation Mechanism. In general, the present results serve to confirm that the major toluene oxidation products predicted by the MCM⁴ are indeed experimentally observed at O₂ concentrations and total pressures similar to those of the atmosphere. The present results are consistent with the majority of previous experimental studies which suggest the dominance of the ring scission products in the primary OH-initiated oxidation of toluene. The present results are also consistent with an emerging quantitative consensus for the yield of cresol (about 20%, as suggested by Noda et al.⁷). In particular, the present experiments have shown that the toluene oxidation mechanism is very sensitive to O₂ concentration, which is a manifestation of the importance of the bicyclic peroxy radical in forming many of the species shown in Figure 3. However, the present experiments have also shown that the methylhexadienedial⁸ and epoxide^{8,31} species, only tentatively identified in a few previous experiments, are significant toluene oxidation products, even though they are somewhat disfavored by the high O₂ concentrations characteristic of the troposphere.

The NO concentration dependence results provide the most important new insights on the toluene oxidation mechanism. The MCM predicts that the dominant fate of the bicyclic peroxy radical under atmospheric and the usual environmental chamber conditions is reaction with NO to form the bicyclic alkoxy radical that goes on to scission to form the butenedial (and methylglyoxal) and methylbutenedial (and glyoxal) products; this reaction also accomplishes the important NO to NO₂ conversion that is characteristic of mechanisms that contribute to tropospheric ozone production. Our results suggest that significant bicyclic peroxy radical reactivity may exist in the absence of NO. Under our experimental conditions, additional NO does serve to change the quantitative product yields somewhat, but it does not significantly change the overall qualitative product distribution. Figure 7 indicates that this reactivity remains high at relatively low initial radical concentrations. In Figure 3, we suggest several other reactive pathways for the bicyclic peroxy radical that attempt to rationalize the observed products under NO_x-free conditions, as well as the observation of stable bicyclic species and OH regeneration. In particular, we propose that peroxy-peroxy reactions are re-

sponsible for the observed reactivity of the bicyclic peroxy radicals under NO_x-free conditions. By analogy to the results obtained for the products formed from the self-reactions of alkene-derived peroxy radicals³²



and from the reactions of acetyl peroxy radicals with the hydroperoxy radical^{33,34}



we propose several possible NO_x-free reaction pathways for the bicyclic peroxy radical in Figure 3. We also include the possible reaction with the toluene-OH adduct suggested by Jenkin et al.²⁴ in Figure 3, although this species is likely to be present only at low concentration at the O₂ concentrations required for significant bicyclic peroxy radical concentrations. While reactions similar to reactions 6–9 are included in the current MCM for toluene, reactions similar to 10 and 11 are not. Since some HO₂ is initially present as a byproduct of the OH source used in our experiments and HO₂ is produced by many of the individual reactions shown in Figures 2 and 3, HO₂ concentrations are likely to be higher than bicyclic peroxy radical concentrations under our experimental conditions (and this is also certainly true of the atmosphere as well). Further, RO₂ + HO₂ rate constants tend to be larger than RO₂ + R'O₂ rate constants (by about a factor of 20 for secondary peroxy radicals such as the bicyclic peroxy radical).³² Thus, it appears that RO₂ + HO₂ reactions are more likely to be important in the present toluene oxidation system than are RO₂ + R'O₂ reactions. We note that the observation of the bicyclic peroxide in our experiments directly indicates that at least some of the bicyclic peroxy radical reactivity is due to HO₂ reaction. Indeed, reactions 9 and 11 can account for all of the bicyclic peroxy radical reactivity and the resulting observed products under NO_x-free conditions and can explain the presence of OH regeneration as follows: (1) the bicyclic peroxide product is produced directly via reaction 9 and (2) the butenedial (and methylbutenedial), bicyclic carbonyl, and OH products are formed via reaction 11.

In the NO Dependence of Relative Product Yields section, we estimated that the bicyclic peroxy radical reactions that did not involve NO were characterized by a lifetime of about 200 ms under certain flow tube conditions. If the generic RO₂ + HO₂ rate constant used in the MCM (2.3 × 10⁻¹¹ cm³ molecule⁻¹ s⁻¹) is assumed to be valid for the bicyclic peroxy radical, an HO₂ concentration of about 2 × 10¹¹ molecules cm⁻³ would be required to rationalize the bicyclic peroxy radical lifetime. Since the total product formation in this experiment was about 2 × 10¹¹ molecules cm⁻³, the estimated HO₂ concentration is roughly consistent with that which would be expected under these conditions.

For the OH scavenger experiments, it was estimated that the OH production rate was about 1 × 10¹¹ molecules cm⁻³ s⁻¹. This OH production rate and the effective RO₂ and HO₂ concentrations can be used to calculate the rate constant for

reaction 11. However, since the scavenger was added after the toluene oxidation system had 50 ms to react, it is even more difficult to estimate the relevant RO₂ and HO₂ concentrations than it is for the early stages of the toluene oxidation process. However, if a value for both species of 1×10^{11} molecules cm⁻³ is assumed, the inferred rate constant for reaction 11 is about 1×10^{-11} cm³ molecule⁻¹ s⁻¹, which is a significant fraction of the generic RO₂ + HO₂ rate constant used in the MCM. While the calculations are somewhat speculative, they do provide quantitative support for the supposition that reaction 11 is potentially a major reaction pathway for bicyclic peroxy radicals under our experimental conditions. Further, since reaction 11 is also one of the proposed routes by which methylbutenedial forms under NO_x-free conditions, the large product yield of this species also provides support for the hypothesis that reaction 11 is a major reaction pathway for the bicyclic peroxy radical.

As discussed in the Introduction, when tested against the results of environmental chamber experiments for the photo-oxidation of toluene, the MCM seems to be missing processes that regenerate OH with little NO to NO₂ conversion.^{4,5} Our results suggest that, at least at high HO₂ and/or low NO concentrations, RO₂ + HO₂ reactions involving the bicyclic peroxy radical can be competitive with the RO₂ + NO reactions that facilitate NO to NO₂ conversion. Therefore, it seems possible, particularly for experimental conditions of high HO₂ and/or low NO, that the environmental chamber results may have been affected by RO₂ + HO₂ reactions. Further, since reaction 11 also produces OH, it can also explain the environmental chamber observation of significant OH regeneration.

The proposed RO₂ + HO₂ reaction pathway might also be important in the oxidation of toluene in the atmosphere. For example, it is well-known that isoprene oxidation chemistry in the atmosphere is dominated by RO₂ + HO₂ chemistry under low NO_x conditions, while RO₂ + NO chemistry dominates at high NO_x conditions.³⁵ However, since aromatic compounds are largely anthropogenic in origin, while isoprene is almost exclusively biogenic in origin, high aromatic concentrations will be more often accompanied by high NO concentrations, whereas high isoprene concentrations are often accompanied by low NO concentrations. Nonetheless, if high enough HO₂/NO ratios exist for certain atmospheric aromatic oxidation conditions, it is possible that RO₂ + HO₂ reactions could be important. In order to determine what HO₂/NO ratios are necessary for these reactions to be important in the atmosphere, it will likely be necessary to experimentally determine the specific rate constants for the RO₂ + HO₂ and RO₂ + NO reactions for toluene-derived bicyclic peroxy radicals.

Acknowledgment. This material is based upon work supported by the National Science Foundation under Grant No. 0753103.

References and Notes

(1) In *The mechanisms of atmospheric oxidation of aromatic hydrocarbons*; Calvert, J. G., Atkinson, R., Becker, K. H., Kamens, R. M.,

Seinfeld, J. H., Wallington, T. J., Yarwood, G., Eds.; Oxford University Press: Oxford, U.K., 2002.

(2) Offenberg, J. H.; Lewis, C. W.; Lewandowski, M.; Jaoui, M.; Kleindienst, T. E.; Edney, E. O. *Environ. Sci. Technol.* **2007**, *41*, 3972.

(3) Velasco, E.; Lamb, B.; Westberg, H.; Allwine, E.; Sosa, G.; Arriaga-Colina, J. L.; Jobson, B. T.; Alexander, M. L.; Prazeller, P.; Knighton, W. B.; Rogers, T. M.; Grutter, M.; Herndon, S. C.; Kolb, C. E.; Zavala, M.; de Foy, B.; Volkamer, R.; Molina, L. T.; Molina, M. J. *J. Atmos. Chem. Phys.* **2007**, *7*, 329.

(4) Bloss, C.; Wagner, V.; Jenkin, M. E.; Volkamer, R.; Bloss, W. J.; Lee, J. D.; Heard, D. E.; Wirtz, K.; Martin-Reviejo, M.; Rea, G.; Wenger, J. C.; Pilling, M. J. *Atmos. Chem. Phys.* **2005**, *5*, 641.

(5) Wagner, V.; Jenkin, M. E.; Saunders, S. M.; Stanton, J.; Wirtz, K.; Pilling, M. J. *Atmos. Chem. Phys.* **2003**, *3*, 89.

(6) Arey, J.; Obermeyer, G.; Aschmann, S. M.; Chattopadhyay, S.; Cusick, R. D.; Atkinson, R. *Environ. Sci. Technol.* **2009**, *43*, 683.

(7) Noda, J.; Volkamer, R.; Molina, M. J. *J. Phys. Chem. A* **2009**, *113*, 9658.

(8) Baltaretu, C. O.; Lichtman, E. I.; Hadler, A. B.; Elrod, M. J. *J. Phys. Chem. A* **2009**, *113*, 221.

(9) Volkamer, R.; Platt, U.; Wirtz, K. *J. Phys. Chem. A* **2001**, *105*, 7865.

(10) Moschonas, N.; Danalatos, D.; Glavas, S. *Atmos. Environ.* **1999**, *33*, 111.

(11) Klotz, B.; Sorensen, S.; Barnes, I.; Becker, K. H. *J. Phys. Chem. A* **1998**, *102*, 10289.

(12) Smith, D. F.; McIver, C. D.; Kleindienst, T. E. *J. Atmos. Chem.* **1998**, *30*, 209.

(13) Becker, K. H.; Barnes, I.; Bierbach, A.; Brockmann, K. J.; Kirchner, F. *Chemical processes in atmospheric oxidation*; Springer-Verlag: Berlin, Germany, 1997; pp 79–90.

(14) Seuwen, R.; Warneck, P. *Int. J. Chem. Kinet.* **1996**, *28*, 315.

(15) Atkinson, R.; Arey, J.; Tuazon, E. C.; Aschmann, S. M.; Bridier, I. *Experimental Investigation of the Atmospheric Chemistry of Aromatic Hydrocarbons and Long-Chain Alkanes*, (ARB-R-94/550; Order No. PB95 109591); Statewide Air Pollution Res. Cent., California University: Riverside, CA, 1994.

(16) Atkinson, R.; Aschmann, S. M.; Arey, J.; Carter, W. P. L. *Int. J. Chem. Kinet.* **1989**, *21*, 801.

(17) Dumdei, B. E.; Kenny, D. V.; Shepson, P. B.; Kleindienst, T. E. *Environ. Sci. Technol.* **1988**, *22*, 383.

(18) Tuazon, E. C.; MacLeod, H.; Atkinson, R.; Carter, W. P. L. *Environ. Sci. Technol.* **1986**, *20*, 383.

(19) Gery, M. W.; Fox, D. L.; Jeffries, H. E.; Stockburger, L.; Weathers, W. S. *Int. J. Chem. Kinet.* **1985**, *17*, 931.

(20) Bandow, H.; Washida, N.; Akimoto, H. *Bull. Chem. Soc. Jpn.* **1985**, *58*, 2531.

(21) Shepson, P. B.; Edney, E. O.; Corse, E. W. *J. Phys. Chem.* **1984**, *88*, 4122.

(22) Glowacki, D. R.; Wang, L.; Pilling, M. J. *J. Phys. Chem. A* **2009**, *113*, 5385.

(23) Bohn, B. *J. Phys. Chem. A* **2001**, *105*, 6092.

(24) Jenkin, M. E.; Glowacki, D. R.; Rickard, A. R.; Pilling, M. J. *J. Phys. Chem. A* **2009**, *113*, 8136.

(25) NIST Chemical Kinetics Database <http://kinetics.nist.gov/kinetics/index.jsp> (accessed June 2010).

(26) Miller, A. M.; Yeung, L. Y.; Kiep, A. C.; Elrod, M. J. *Phys. Chem. Chem. Phys.* **2004**, *6*, 3402.

(27) Seeley, J. V.; Meads, R. F.; Elrod, M. J.; Molina, M. J. *J. Phys. Chem. Chem. Phys.* **1996**, *100*, 4026.

(28) Frankcombe, T. J. *J. Phys. Chem. A* **2008**, *112*, 1572.

(29) Zhao, J.; Zhang, R.; Misawa, K.; Shibuya, K. *J. Photochem. Photobiol., B* **2005**, *176*, 199.

(30) Berndt, T.; Böge, O. *Phys. Chem. Chem. Phys.* **2001**, *3*, 4946.

(31) Yu, J.; Jeffries, H. E. *Atmos. Environ.* **1997**, *31*, 2281.

(32) Jenkin, M. E.; Hayman, G. D. *J. Chem. Soc. Faraday Trans.* **1995**, *91*, 1911.

(33) Hasson, A. S.; Tyndall, G. S.; Orlando, J. J. *J. Phys. Chem. A* **2004**, *108*, 5979.

(34) Dillon, T. J.; Crowley, J. N. *Atmos. Chem. Phys.* **2008**, *8*, 4877.

(35) Paulot, F.; Crouse, J. D.; Kjaergaard, H. G.; Kürten, A.; St. Clair, J. M.; Seinfeld, J. H.; Wennberg, P. O. *Science* **2009**, *325*, 730.

JP105467E